Journal Pre-proofs

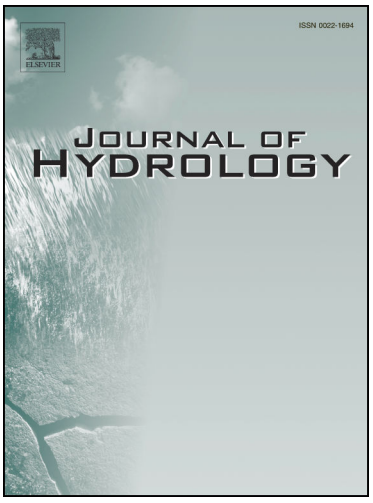

Research papers

Modelling the impact of runoff generation on agricultural and urban phosphorus loading of the subtropical Poyang Lake (China)

Sanyuan Jiang, Qi Zhang, Adrian D. Werner, Christopher Wellen, Peng Hu, Jinhua Sun, Yanqing Deng, Michael Rode

PII: S0022-1694(20)30950-1
DOI: https://doi.org/10.1016/j.jhydrol.2020.125490
Reference: HYDROL 125490

To appear in: *Journal of Hydrology*

Received Date: 31 March 2020
Revised Date: 15 July 2020
Accepted Date: 29 August 2020

Please cite this article as: Jiang, S., Zhang, Q., Werner, A.D., Wellen, C., Hu, P., Sun, J., Deng, Y., Rode, M., Modelling the impact of runoff generation on agricultural and urban phosphorus loading of the subtropical Poyang Lake (China), *Journal of Hydrology* (2020), doi: https://doi.org/10.1016/j.jhydrol.2020.125490

Modelling the impact of runoff generation on agricultural and urban phosphorus loading of the subtropical Poyang Lake (China)

Sanyuan Jiang[1], Qi Zhang[1*], Adrian D. Werner[2], Christopher Wellen[3], Peng Hu[4], Jinhua Sun[5], Yanqing Deng[6], Michael Rode[7]

[1]Key Laboratory of Watershed Geographic Sciences, Nanjing Institute of Geography and Limnology, Chinese Academy of Sciences,73 East Beijing Road, 210008, Nanjing, China
[2]College of Science and Engineering, and National Centre for Groundwater Research and Training, Flinders University, GPO Box 2100, Adelaide, SA 5001, Australia
[3]Department of Geography and Environmental Studies, Ryerson University, Toronto, 350 Victoria Street Ontario, Canada
[4]State Key Laboratory of Simulation and Regulation of Water Cycle in River Basin, China Institute of Water Resources and Hydropower Research, A-1 Fuxing Road, Haidian District, 100038 Beijing, China
[5]State Key Laboratory of Hydrology and Water Resources and Hydraulic Engineering Science, Nanjing Hydraulic Research Institute, 223 Guangzhou Road, 210029, Nanjing, China
[6]Jiangxi province Hydrology Bureau, 1499 Jiangnan Street, Xihu District, 330008 Nanchang, China
[7]Department of Aquatic Ecosystem Analysis and Management, Helmholtz Centre for Environmental Research-UFZ, 39114, Magdeburg, Germany

[*]Corresponding author: Qi Zhang (qzhang@niglas.ac.cn)

Originally submitted to *Journal of Hydrology* on March 31, 2020

Revision submitted to *Journal of Hydrology* on July 15, 2020

Abstract

Water quality degradation and eutrophication in surface water bodies caused by excessive phosphorus loads from agriculture and urbanisation are widespread problems. Although phosphorus (P) is often the limiting factor of aquatic ecosystems, only few studies have characterised the primary factors that influence P export in subtropical monsoon catchments. This study aims to assess the temporal and spatial variations in P fluxes, and to investigate the factors controlling P export in a subtropical catchment. Runoff and P export in the Le An River catchment, which flow to Poyang Lake (China) were evaluated using the HYPE model. Sensitivity analysis and calibration of hydrological and P transport parameters were undertaken using PEST. Results show that: (a) HYPE reproduced sufficiently well ($NSE \geq 0.73$, $|PBIAS| \leq 14.5\%$) the stream flow dynamics for widely varying climatic conditions and across six sub-catchments of contrasting physiographic characteristics; (b) HYPE captured intra-annual patterns of total P (TP) loads, although with overestimation of annual TP loads by 8.5-47.0% across two monitoring sites; (c) TP loads had the ranges between 0.24-0.88 kg/ha/yr and 4.31-4.69 kg/ha/yr from forest-dominant upstream areas and the downstream plains region, respectively, with the latter being more urbanised and having higher percentage of agriculture; (d) Soil erosion from surface runoff and adsorption/desorption of soil P are the main factors controlled P export from the catchment; (e) most P export occurred during March-August when rainfall-runoff is highest and agricultural practices are most active; (f) stream TP concentrations were greatly affected by point source inputs, especially during low-flow conditions in downstream plains region. This study indicates that measures to reduce TP export to receiving water bodies in subtropical monsoon areas, like Poyang Lake, should focus on managing diffuse sources from soil erosion and surface runoff etc., whereas improvements to sewage management is more likely to reduce river TP concentrations during low-flow periods.

Keywords: Phosphorus export; Rainfall-runoff; Sensitivity analysis; HYPE; Catchment model; Nutrient loads

1. Introduction

Excessive nutrient export from watersheds causes elevated nutrient concentrations in surface waters, particularly receiving water bodies, leading to water quality deterioration, eutrophication, and biodiversity loss (Duan et al., 2008; Gurung et al., 2013; Kaye et al., 2006; Moore et al., 2008; Rodríguez-Blanco et al., 2013; Zhang et al., 2019). Elevated concentrations of the nutrients phosphorus (P) and nitrogen (N) are the most common causes of eutrophication in freshwater ecosystems, such as lakes, reservoirs, streams, and the upper reaches of estuarine systems (Conley et al., 2009; Correll, 1999; Edwards and Chambers, 2002; Santos et al., 2015; Smith et al., 1999). P export from soils to surface water bodies occurs not only in the form of particulate P (PP) attached to eroded surface soil, but also as dissolved P (DP) (Gao et al., 2017; Garnache et al., 2016; Hansen et al., 2002; Seitzinger et al., 2005; Tang et al., 2008). During the transport of P from watersheds to receiving water bodies, DP and PP fractions may continuously change as a result of in-stream processes. These processes include uptake of DP by aquatic biota, transformations between PP and DP caused by changes in the equilibrium DP concentration, deposition of suspended PP, and re-suspension of streambed or streambank PP (Bitschofsky and Nausch, 2019; Edwards et al., 2000).

Diffuse and point sources of P export are usually differentiated in studies of the origins of stream P (e.g., Correll, 1999; Duan et al., 2008; Garnache et al., 2016). Diffuse P export at the catchment scale, such as through runoff and erosion following rainfall from agricultural fields and fertilized lawns and gardens in urban areas, is influenced by many factors. These include the spatial and temporal characteristics of nutrient sources, physiographic properties, climatic patterns, hydrological conditions and agricultural management practices (Cao et al., 2014; Duan et al., 2008; Hunsaker and Johnson, 2017; Jiang et al., 2015; Jin et al., 2018; Kim et al., 2006;

Lazzarotto et al., 2005; Song et al., 2014; Sun et al., 2011). The application of fertilisers, including manure, within agricultural settings is usually identified as the main diffuse sources of P to surface waters (Brendel et al., 2019; Carpenter et al., 1998; EEA, 2010; Lam et al., 2012; Rode et al., 2008). Diffuse P sources were estimated to contribute up to 93% of total P loads within rivers in China, with contribution from agricultural diffuse sources accounting for 85% (Ongley et al., 2010). Thus, identification of major factors that influence P export from catchments dominated by diffuse P sources has become a critical component of watershed management, in particular where P pollution issues have arisen, such as in subtropical regions of China (Chen and Lu, 2014; Li et al., 2008; Wang et al., 2020).

Previous studies demonstrate that stream TP concentrations and mass fluxes are often correlated to the percentage of land use dedicated to agriculture (Gurung et al., 2013; Lu et al., 2017; Wang et al., 2014). Agricultural practices can lead to greater soil erosion, which enhances P transport through particulate entrainment in the runoff that occurs under high rainfall intensities, contributing to increased stream PP concentrations (Kim et al., 2018; Rodríguez-Blanco et al., 2013; Sandstroem et al., 2020; Song et al., 2014; Sun et al., 2011; Yang et al., 2009). The urban landscape may also serve as a strong diffuse source of P to the aquatic environment, due to increased impervious cover creating more overland flow and sediment-bound P transport as well as the release of chemicals (e.g., detergents) to waterways (Arnold and Gibbons, 1996; Duval, 2018; Gurung et al., 2013). Rainfall imposes complex effects on diffuse P concentrations because it can dilute P concentrations in streams and downstream lakes, but high rainfall can also cause runoff and soil erosion from agriculture, where inorganic P may be adsorbed onto eroding sediment (Bender et al., 2018; Garnache et al., 2016). P export from point sources most commonly includes the release of wastewaters from sewage treatment plants, municipal and

industrial sites, as well as rural point sources such as feedlots (Garnache et al., 2016; Lam et al., 2012; Palmer-Felgate et al., 2010; Schoumans et al., 2014).

Numerous catchment modelling studies have been undertaken to simulate runoff and P export, and to predict the influence of climate change and anthropogenic activities on catchment hydrology and nutrient discharge. Popular catchment models used to simulate runoff and P export include SWAT (Arnold et al., 1998), AGNPS/AnnAGNPS (Bingner et al., 2012), INCA-P (Wade et al., 2002), SPARROW (Schwarz et al., 2006), HSPF (Donigian et al., 1995) and HYPE (Lindström et al., 2010). Among these models, SWAT is the most widely used model (e.g., Lai et al., 2006; Panagopoulos et al., 2011; Trindade et al., 2010; Wang et al., 2012; Wellen et al., 2015; Xu and Peng, 2013). HYPE has also been used extensively, including for the simulation of runoff and P export from temperate watersheds of various scales (Jiang et al., 2012; Lindström et al., 2010; Strömqvist et al., 2012; Yin et al., 2016). The physically based HYPE model represents a compromise between highly parameterised models like SWAT and HSPF and much simpler statistical models like SPARROW. It simulates stream flow with the commonly available and easily measurable meteorological data of time series precipitation and air temperature. HYPE keeps good balance between model complexity, representation of internal hydrological and biogeochemical processes, as well as input data availability. Thus, it is suitable for usage in meso- to large scale catchments (e.g., Jiang et al., 2014; Lindström et al., 2010; Strömqvist et al., 2012; Yin et al., 2016).

Catchment modelling studies of P transport rarely involve subtropical or tropical monsoon regions, where runoff characteristics differ to those of temperate areas due to contrasting meteorological patterns, hydrological regimes, and cropping systems (e.g., Li et al., 2015; Li et

al., 2017; Trindade et al., 2010; Xu and Peng, 2013). Examples of P transport modelling studies in subtropical/tropical monsoonal regions include: SWAT simulation of stream flow and diffuse P export from an upstream watershed of the Dongjiang River in southern China (Xu and Peng, 2013); SWAT modelling of diffuse P loads from a small catchment in southeastern Brazil (Trindade et al., 2010); application of the INCA model to simulate stream flow and P concentrations of the Mahanadi River affected by both point and diffuse sources in India (Jin et al., 2018); simulation of stream flow and diffuse P export from Xitiaoxi watershed in China using HSPF (Li et al., 2017); modelling of stream flow and diffuse nutrient export from Zhongtian River watershed in China by AnnAGNPS (Li et al., 2015); and simulation of phosphorus transport in a headwater catchment in the upper Taihu Lake Basin, China using SPARROW (Zhang et al., 2019). Of these modelling studies, only Jin et al. (2018) attempt to investigate the effect of changes in both point source (e.g., due to higher population growth and increased treated sewage discharge) and non-point (e.g., land use change and enhanced atmospheric deposition) sources of P on stream water quality and P loads.

In this study, P export from the subtropical Le An River catchment, southeast China, is investigated. This catchment provides significant input to China's largest freshwater lake, i.e., Poyang Lake. Poyang Lake is connected to the Yangtze River through one of the few remaining natural channels of its type in China. The lake provides habitat for around half a million migratory birds and the vulnerable Finless Porpoise, and also plays a significant role in regulating floods in the Yangtze River (Dong, 2012; Wang et al., 2013; Zhang et al., 2014). It receives most of its inflow from five rivers (i.e., the Ganjiang, Fuhe, Raohe, Xinjiang, and Xiushui Rivers), which contribute significant nutrient loads to the lake. Water quality in the lake and rivers (within Poyang Lake's catchment) has deteriorated since the 1980s in the face of increasing population,

economic growth, rapid urbanization, and changing climatic-hydrological regimes (Wu et al., 2018; Zhang et al., 2014). Jiang et al. (2017) identified farmland and urban areas as the main source of heavy metal pollution in the Le An River based on Pearson's correlation analysis between land use types and the concentrations of trace metals. They concluded that forests and grassland were sinks for dissolved trace metals (Jiang et al., 2017). However, stream nutrient concentrations and nutrient fluxes in the Le An River catchment have not been investigated previously. Other studies of P export into Poyang Lake include the investigation of Wang et al. (2008), who used systematic monitoring to conclude that agricultural drainage water, urban sewage and groundwater are the main drivers of N and P loads in tributaries and the lake. Deng et al. (2011) analysed the trade-off between economic growth and the reduction of N and P loads within the Poyang Lake Basin. They found that restricting N and P outputs from sectors with the highest levels of discharge is more effective for balancing economic growth and the reduction of N and P loads than restricting N and P loads from all sectors. None of the previous P export studies in the Poyang Lake Basin have investigated variations in P loads in the context of the contributing factors, which should be determined to support decision making to reduce nutrient loads.

The objectives of this study are to assess the temporal and spatial variations in P fluxes in subtropical monsoon catchment, and to investigate the major factors influencing P export at the catchment scale. To accomplish these goals, HYPE, a semi-distributed physically based model that runs on daily time steps, is applied at the Le An River catchment, along with the parameter estimation code PEST to undertake sensitivity analysis and calibration of hydrology and P transport parameters. The results of the current analysis will add to previous investigations of P transport within subtropical monsoon areas by exploring the effects of land use, rainfall patterns

and both diffuse and point sources of P on stream P concentrations and P fluxes. This study is expected to assist in decision making for catchment P management, taking into account river ecosystem responses to P loading.

2. Materials and methods

2.1 Study area and data availability

The Le An River catchment (coordinates: 28°55′41″-29°1′21″N, 116°29′35″-117°48′24″E) is located in Jiangxi Province, China (Figure 1a), and has a total area of 8324 km^2 (Jiang et al., 2017). The catchment is dominated by mountainous regions in the northeast and plains region in the southwest, which differ in terms of topography, land use, and soil type, as shown in Figure 1. A summary of the main physiographic and land use characteristics of the Le An River catchment is provided in Table 1.

Figure 1 near here

Table 1. Summary of physiographic and land use characteristics of the Le An River catchment. Hilly/mountainous areas and plains region are those at elevations greater or less than (respectively) 90 m.

Characteristics	**Categories (% area)**
Topography (% coverage)	Mountainous areas: 90 – 1596 m (70%), Plains region: 13 – 90 m (30%)
Land use (% coverage)	Forest (74.5%), arable land (19.0%), grassland (2.6%), urban area (1.6%), water bodies (1.6%), others (0.7%)
Soil (texture, % coverage)	Red soil (loam and clay, 64.0%), paddy soil (silty clay, 18.4%), yellow-red soil (clay and loam, 10.5%), brown soil (loam, 2.4%), yellow soil (loam and clay, 2.1%), grey alluvial soil (loam and clay, 1.5%), yellow-brown soil (loam, 0.4%), volcanic ash soil (clay, 0.5%), neutral purple soil (silty clay loam, 0.2%)
Arable land (% coverage)	Paddy field (79.0%), dry land (17.5%), vegetable land (3.5%)

A Digital Elevation Model (DEM) of the Le An River catchment was downloaded from the NASA Shuttle Radar Topographic Mission (SRTM, http://srtm.csi.cgiar.org/) with grid resolution of 90 m (Figure 1b). Land surface elevations vary between 13 m and 1596 m (above sea level). Land use was obtained from the Geographical Information Monitoring Cloud Platform of China (http://www.dsac.cn/, Figure 1c) for the year 2000 with grid resolution of 250 m. The percentages of coverage of six land use types are listed in Table 1. Forests dominate land use in mountainous areas, whereas the plains region are mainly covered by arable lands and urban areas (Figure 1b). Double-cropping rice is the dominant crop type, and is sown mainly in the plains region. Early rice is sown in middle April and harvested in late July, while late rice is sown in late July and harvested in October/November. The distribution of soil in the catchment was obtained from a soil survey conducted by the Institute of Soil Sciences, Chinese Academy of Sciences, with nine types of soil categorized according to the Genetic Soil Classification of China (Figure 1d). Red soil and paddy soil are the dominant types of soil, making up 64% and 18.4%, respectively of the total catchment area (Table 1).

Daily rainfall measurements were obtained from 44 meteorological stations within the Le An River catchment, which experiences a subtropical monsoon climate characteristed by moderate temperature differences between summer and winter. The average temperature during 1960-2008 was 17.6 ℃, with June-August average of 27.3 ℃ and December-February average of 7.1 ℃, showing general increases from moutainous areas to the plains region due to altitude effects (Zhang et al., 2014). Average annual precipitation for the period of 1960-2012 was 1626 mm, of which more than 50% falls during March-June, with the largest monthly totals usually occuring in June (Li and Hu, 2019). Seasonal variations in stream flow reflect rainfall patterns, whereby

the highest flows usually occur in March-June, whereas stream flow during December-February is generally the lowest.

Stream flow and stream P concentrations are measured at the stream gauging stations shown in Figure 1b. For water quality analysis, single grab samples were collected and analyzed as part of the current study at weekly to three-monthly intervals during 2009-2011 and 2016 (Table 2). For laboratory analysis of stream P concentrations, 5 L stream water samples were collected from 50 cm below the water surface, and these were kept in acid-cleaned, sealed containers and transferred to the laboratory under cool and shaded conditions following the method of sample collection defined by Wu et al. (2018). Water samples used to determine DP concentrations were filtered using 0.45-micron membrane filters in the field. DP concentrations were determined from a UV spectrophotometer using the molybdenum blue method, as adopted by Wu et al. (2018). TP concentrations were analyzed using persulfate digestion and ion chromatography following the methods described by De Borba et al. (2014). PP concentrations equal the difference between concentrations of TP and DP. Available stream flow and stream P measurements are summarized in Table 2.

Table 2. Available stream flow and stream P measurements in the Le An River catchment. See Figure 1 for station locations.

Variables	Stations	Frequency	Parameters	Period
Stream flow	Wang Kou, San Du, Yin Shan	Daily	Discharge (m^3/s)	1977-1986
	Xiang Tun, Hu Shan, and Shi Zhen Jie	Daily	Discharge (m^3/s)	1977-1986 2009-2011
Stream P concentration	WQ1, WQ2, WQ5	Three-monthly	TP, DP (mg/L)	2009-2011
	WQ3, WQ4, WQ6	Monthly	TP (mg/L)	2009-2011

	WQ3, WQ6	Biweekly to weekly	TP, DP (mg/L)	2016

2.2 Hydrological and phosphorus-export model, HYPE

HYPE is a semi-distributed process-oriented catchment model that simulates hydrology and nutrient export at daily time steps (Lindström et al., 2010). HYPE simulates evapotranspiration, surface runoff, infiltration, macropore flow, percolation, interflow, regional groundwater flow, and river flow (Lindström et al., 2010). In applying the HYPE model, a catchment is first delineated into sub-basins based on topography and the stream network. Each sub-basin is further classified into different Soil-Land use Classes (SLCs). Each SLC represents a so-called Hydrological Response Unit (HRU). The soil is divided into a maximum of three layers, within which hydrological and nutrient transformation processes are simulated. The SLCs are not coupled to geographic locations but are defined as fractions of a sub-basin area. A detailed description of the model processes and governing equations of HYPE is provided by Lindström et al. (2010).

Within HYPE, sources of P input to the soil include diffuse sources from applied organic and inorganic fertiliser, manure, plant residues, atmospheric deposition, and rural household diffuse sources (Lindström et al., 2010). In HYPE, the mass of P stored in the soil is split into several fractions (Lindström et al., 2010), namely: organic P with slow transformation (humusP), organic P with rapid transformation (fastP), adsorbed inorganic P (partP), and dissolved P (DP). The terrestrial processes influencing P export and concentration in HYPE include degradation, mineralization, adsorption/desorption, plant uptake and soil erosion (Lindström et al., 2010; Morgan, 2001). In-stream processes include sedimentation, re-suspension, primary production

and mineralization (Lindström et al., 2010). Sources of point P input from urban and industrial activities (e.g., sewage treatment works) are added to the river to which the effluent is discharged.

The equilibrium between soil DP and PP is governed by adsorption/desorption, which is calculated using the Freundlich isotherm (Lindström et al., 2010):

$$F_{PADS} = p_{PADS}\left(p_{FRCO}\left(C_{SPEQ}\right)^{p_{FREX}} c_{SLAY} c_{BULKD} - X_{PARTP}\right) \quad (1)$$

where F_{PADS} is the amount of adsorbed/desorbed P (kg/km^2/d), p_{PADS} is the adsorption/desorption rate that is dependent on soil type (1/d), p_{FRCO} is the coefficient in the Freundlich equation related to adsorption/desorption that is dependent on soil type (1/kg), C_{SPEQ} is the SP equilibrium concentration in the Freundlich equation related to desorption (mg/L), p_{FREX} is the exponent in the Freundlich equation related to adsorption/desorption that is dependent on soil type (-), c_{SLAY} is the soil layer thickness (m), c_{BULKD} is soil bulk density, taken as 1300 kg/m^3, and X_{PARTP} is the mass of partP (kg/km^2). The above parameters related to P mass are given as area-specific values, such that multiplication by the SLC area (km^2) produces total P mass for an SLC.

2.3 Model setup and estimation of P loads

The Le An River catchment was delineated into 71 sub-basins, which range in area from 0.03 to 423 km^2 (average 117 km^2). Subsequently, 47 SLCs were classified by overlaying maps of soil and land use. The input data for the HYPE model, consisting of daily rainfall and temperature, were interpolated using measurements from available meteorological stations located within or nearby the respective sub-basins (Figure 1b). HYPE was run for a calibration period of five years (1 Jan 1978 to 31 Dec 1982) using daily discharge observed from six discharge gauging stations (i.e., Wang Kou, San Du, Xiang Tun, Yin Shan, Hu Shan and Shi Zhen Jie; Figure 1b). Stream

flow validation consisted of two periods, namely a four-year period from 1 Jan 1983 to 31 Dec 1986 using daily stream flow measurements from the six gauging stations, and a three-year period from 1st Jan 2009 to 31st Dec 2011 using daily stream flow observations from three stations (Xiang Tun, Hu Shan and Shi Zhen Jie; Figure 1b).

Sources of P input to HYPE included agricultural inputs (mineral fertiliser and manure application), atmospheric deposition, and point inputs (wastewaters from sewage treatment plants). Initial soil P contents (i.e., humusP, fastP, and partP) also needed to be estimated. These were derived from statistical data, field surveys and published literature (Hu, 2010; Jiang et al., 2017; Jiao et al., 2010; Liu et al., 2013). In agricultural lands within the study area, fertiliser application rates fall in the range 75-344 kg/ha/yr for N and 38-150 kg/ha/yr for P (Jiang et al., 2017). Point sources discharging to rivers were defined based on recordings of daily average discharge of wastewater to rivers and TP concentrations of the effluent (locations of wastewater treatment plants are shown in Figure 1b), which are available from local Water Affairs Bureaus. All the available stream TP and DP measurements for the period 1 Jan 2009 - 31 Dec 2011, and PP estimates (TP minus DP) were used for calibration of P export-process parameters.

Plausible initial values and ranges of HYPE model parameters representing the conditions encountered in the Le An River catchment are given in Table 3. These were defined based on knowledge of hydrological and P transformation processes, literature review, and with referrence to published HYPE applications in other catchments (Jiang and Rode, 2012; Jiang et al., 2014 and 2019; Jomaa et al., 2016; Lindström et al., 2010; Strömqvist et al., 2012; Yin et al., 2016).

Table 3. Physical meaning, initial value and range, RCS (Relative Composite Sensitivity), and optimized value of the HYPE parameters for simulating flow and P transport in the Le An River catchment.

Parameter	Categories	Initial value	Range	RCS ×1000	Calibrated value
Hydrological-process parameters					
rrcs1 – Recession coefficient for runoff in the uppermost soil layer (1/d)	Red soil	0.28	0.01-1.0	3.17	0.748
	Paddy soil	0.10	0.01-1.0	0.46	0.366
srrcs – Recession coefficient for saturation-excess surface runoff (1/d)	Arable land	0.12	0.1-1.0	0.38	0.10
	Forest	0.12	0.1-1.0	0.56	0.242
	Grassland	0.30	0.1-1.0	0.07	0.262
	Urban area	0.40	0.1-1.0	0.20	0.114
rivvel – Maximum velocity in the stream channel (m/s)		2.47	0.01-10	2.65	1.58
rcgrw – Recession coefficient for regional groundwater flow (1/d)		0.10	0.001-1.0	0.91	0.026
mperc – Maximum percolation capacity (mm/d)	Red soil	4.0	0.001-100	2.9	18.12
	Paddy soil	2.7	0.001-100	0.009	0.01
Phosphorus-process parameters					
wprod – Production/decay of P in water (kg/m^3/d)		0.002	0.001-1.0	10.70	0.0027
minerfp – Degradation of fastP to SP (1/d)	Arable land	0.50	0.00001-1.0	1.97	0.55
	Forest	0.0003	0.00001-1.0	43.19	0.0005
freund1 – Coefficient in the Freundlich equation (1/kg)	Red soil	190	10-250	101.08	189.98
	Paddy soil	50	10-250	50	12.78
freund2 – Exponent in the Freundlich equation (-)	Red soil	1.1	0.55-1.65	166.04	1.65
	Paddy soil	0.75	0.38-1.13	42.34	1.0
freund3 – Parameter that controls the adsorption/desorption velocity (1/d)	Red soil	0.50	0.25-0.75	17.23	0.75
	Paddy soil	0.009	0.005-0.014	0.17	0.005
sreroexp – Exponent in the equation for the calculation of surface runoff erosion (-)		2.26	1.5-2.6	666	2.28

P loads (*m* in units g/d) were estimated as the product of flow and P concentration, and considering TP (m_{TP}), DP (m_{DP}) and PP (m_{PP}; inferred from the difference between m_{TP} and m_{DP}). Instantaneous *m* values calculated from field measurements were compared to daily *m* values calculated by the numerical model. P loads for longer time steps (e.g., monthly, annual) were obtained from the product of the flow volume and the flow-weighted mean concentration (for a

given time-step length), according to the suggestion of Williams et al. (2015). The equation for annual P loads is given by:

$$m_i = \mathrm{KV}\frac{\sum_{j=1}^{n} Q_j C_{ij}}{\sum_{j=1}^{n} Q_j} \quad (2)$$

where i = TP, DP or PP, K converts time units (86,400 s/d), V is the annual cumulative flow volume (m^3), C_{ij} is the instantaneous concentration (mg/L) of TP, DP or PP (i = 1 to 3, respectively) measured on the jth day, Q_j is the jth daily flow rate (m^3/s) from gauging station data, and n is the number of concentration measurements with the yearly time step. Equation (2) is easily modified to produce results at monthly time steps.

2.4 Sensitivity analysis and calibration

It is common practice to explore the sensitivity of model outputs to changes in parameter values (i.e., 'parameter sensitivity') as an initial evaluation of the performance of catchment models (Beven and Binley, 1992; Doherty, 2016; Xie et al., 2017). This is useful in assessing the role of the many nonlinear calculations in HYPE in parameter-output relationships, and the more general issue of equifinality in watershed simulation, which is valuable for guiding monitoring to aid in constraining model calibration and validation methods (Beven and Binley, 1992; Cuo et al., 2011; Xie et al., 2017). Sensitivity analysis results are used to focus the considerable computational resources needed for calibration on the most sensitive parameters, while insensitive parameters can be assigned reasonable values based on expert knowledge and omitted from the calibration process.

In the current study, PEST was used to undertake sensitivity analyses on the hydrology and P transport parameters of HYPE. Results of sensitivity analyses are listed in Table 3. Parameter sensitivity is expressed as Relative Composite Sensitivity (RCS), given by:

$$RCS = |P|\frac{\Delta O}{\Delta P} \quad (3)$$

where $|P|$ is the magnitude of the parameter value (P), and $\Delta O/\Delta P$ is the parameter's composite sensitivity (Doherty, 2016; Jiang et al., 2014).

Following the identification of sensitive and insensitive hydrology and P transport parameters, the HYPE model was calibrated using PEST in a step-wise, multi-objective manner. This was carried out using the following calibration sequence: (1) hydrology-related parameters were calibrated to obtain optimal agreement between observed and simulated hydrographs; (2)

P-transport parameters were calibrated to obtain optimal agreement between simulated and observed stream TP and DP concentrations, and inferred PP concentrations. PEST optimizes parameters by reducing the discrepancies between field observations and model-generated counterparts, using a weighted least-squares measure (Doherty, 2016):

$$MOF = \sum_{l,n} \omega_i \cdot \left(X_{i,j,sim} - X_{i,j,obs}\right)^2 \quad (4)$$

where *MOF* is the multi-objective function that is minimized through calibration; $X_{i,j,sim}$ and $X_{i,j,obs}$ represent simulated and measured stream parameters (i.e., discharge and TP, DP and PP concentrations), respectively on the *j*th day from the *i*th gauging station; *l* is the total number of gauging stations utilized in calibration; *n* is the total number of days with available stream flow/P measurements at the *i*th gauging station; ω_i represents a weight, calculated as the reciprocal of the standard deviation of stream flow or P measurements from the *i*th gauging station in order to reduce the dominance of large values on the objective function (Doherty, 2016; Jiang et al., 2014).

The commonly used statistical criteria, consisting of *NSE* (Nash-Sutcliffe efficiency), percent bias (*PBIAS*), and the ratio between RMSE (root mean squared error) and the standard deviation of measurements (*RSR*), were used to evaluate model performance in terms of stream flow. Formulae and interpretation of *NSE* and *RSR* can be found in several previous articles (e.g., Dupas et al., 2017; Jiang et al., 2014; Moriasi et al., 2007; Serpa et al., 2017). In assessing simulated P export against measurements, *PBIAS* and *RSR* were used, following suggestions by Rode et al. (2009) and Jackson-Blake et al. (2015). *PBIAS* was determined using:

$$PBIAS = \frac{\sum_{j=1}^{n}(X_{j,sim} - X_{j,obs}) \times 100}{\sum_{j=1}^{n} X_{j,obs}} \quad (5)$$

Where $X_{j,sim}$ and $X_{j,obs}$ are the *j*th simulated and observed values, respectively of the variable being evaluated, and *n* is the total number of observations.

3. Results

3.1 Stream P observations

Stream TP and DP concentrations observed during 2009-2011 from monitoring stations WQ1-WQ6, and during 2016 (stations WQ3 and WQ6) are presented in Figure 2. Both stream TP and DP concentrations display large temporal varaibility, with respective Coefficients of Variation (CVs) of TP at stations WQ1 to WQ6 of 66.0%, 93.8%, 74.0%, 74.9%, 83.6% and 78.0%, respectively. Stream DP concentrations have CVs of 65.7%, 67.9%, 190%, 80.3%, 54.6% and 181% (stations WQ1 to WQ6, respectively). At stations WQ1-WQ5, high stream TP (0.172-0.386 mg/L) and DP (0.068-0.143 mg/L) concentrations occur during storm-flow conditions in July/August. This is most likely due to high rainfall (average monthly rainfall 166.1 mm) and runoff (average monthly runoff 113.8 mm) during this period, leading to mobilization of both PP and DP (e.g., Minaudo et al., 2019). Conversely, at station WQ6, the most downstream station located within the plains region, elevated stream TP and DP concentations were observed under low-flow conditions (October-January), when average monthly rainfall and runoff are 78.1 mm and 29.1 mm, respectively.

The maximum TP and DP concentrations were observed on 13 Nov 2016 from station WQ6 with respective values of 3.06 mg/L and 0.63 mg/L. A similar trend in spatiotemporal patterns of DP (as that observed at WQ6) was reported by Duan et al. (2008), who observed DP concentrations inversely correlated to river flow in subtropical downstream reaches of the Yangtze River (e.g., Datong station, latitude 30.778°, longitude 117.612°). They attributed this behaviour to the

dominance of point sources of P (e.g., sewage from cities) during times of low flow. Minaudo et al. (2019) also illustrated that point P sources largely control the background pollution, through their investigation of seasonal P (TP, DP) concentrations and discharge in 219 French catchments, where flow variations are seasonal resulting in limited dilution capacity during low flows.

Figure 2 near here

Table 4 presents a statistical summary of measured stream TP and DP concentrations from stations WQ1-WQ6 and land use characteristics of the corresponding sub-basins. Stream TP and DP concentrations show spatial variability, characterised by generally lower values in moutainous areas (stations WQ1-WQ3) compared to the plains region (stations WQ4-WQ6). The average proportions of DP in TP (for stations WQ1 to WQ6) ranged from 20.3 (at WQ6) to 58.6% (at WQ4). This indicates that a larger proportion of P is transported in the form of PP with intensive agricultural activities, most likely attributable to greater soil erosion. The higher stream P concentrations in the plains region relative to the mountainous areas are attributed to more intesive human activites on the plains, including: (i) more input from point sources in urban areas, and (ii) larger percentages of arable lands leading to higher diffuse nutrient loads.

Table 4. Statistical summary of stream P (TP, DP, PP) concentrations for monitoring stations WQ1-WQ6 and land use characteristics of the corresponding sub-basins.

Site	**Sub-basin area (km^2)**	**Land use percentage (%)**			**TP concentration (mg/L)**		**DP concentration (mg/L)**		**PP concentration (mg/L)**	
		Forest	Arable land	Urban area	Range	Mean	Range	Mean	Range	Mean
WQ1	18.96	92.5	4.4	0.9	0.015-0.172	0.072	0.007-0.087	0.041	0.003-0.118	0.031
WQ2	37.96	91.3	8.7	0	0.025-0.262	0.073	0.004-0.068	0.031	0.006-0.031	0.012
WQ3	51.09	74.5	18.5	2.3	0.005-0.386	0.046	0.001-0.143	0.012	0.0007-0.243	0.040

WQ4	112.67	60.9	33.8	1.3	0.025-0.228	0.087	0.004-0.135	0.051	0.012-0.151	0.041
WQ5	157.64	58.4	35.3	3.2	0.015-0.253	0.087	0.008-0.089	0.049	0.0004-0.178	0.043
WQ6	184.43	29.7	49.9	5.2	0.020-3.061	0.256	0.003-0.634	0.052	0.02-2.427	0.223

Figure 3 presents log-log plots of observed TP and DP concentrations against instantaneous measurements of *Q* for the stations WQ3 and WQ6, where both flow and water quality monitoring data are available. Godsey et al. (2009) used a similar type of plot to interpret contaminant behaviour at the catchment scale. Stream TP and DP concentrations exhibit less variability than discharge for both stations. For example, the measured stream TP and DP concentrations during low-flow conditions on 7 Nov 2016 were 2.0- and 3.9-times higher than during high-flow conditions on 4 Jun 2016 at station WQ6. Conversely, the observed high flow on 4 Jun 2016 was about 68-times greater than the low flow on 7 Nov 2016 at WQ6. The slopes of concentration-discharge regression lines for WQ6 are negative (i.e., slopes are -0.248, -0.380 and -0.211 for TP, DP and PP, respectively) and statistically significant (i.e., relative to a zero-slope regression) according to the traditional P value ($P < 0.05$). Thus, according to the criteria proposed by Godsey et al. (2009), the downstream site exhibited nearly chemostatic behaviour for TP and DP, such that dilution played the primary role in P concentration trends. Despite statistical significance, the r^2 values for the regressions were low (<0.13). At station WQ3, TP and DP also exhibited near chemostatic behaviour (especially for DP), although not in a statistically significant manner.

Figure 3 near here

3.2 Calibrated parameters and sensitivities

Table 3 presents the calibration and sensitivity analysis results. The calibrated hydrological parameter values in the study have the same order as those obtained from stream flow modelling of temperate regions with HYPE, such as the Selke catchment in central Germany (Jiang et al., 2014). For example, the recession coefficient for runoff in the uppermost soil layer of paddy soil (*rrcs1*) was 0.366 in the Le An River catchment, while a value of *rrcs1* = 0.104 was obtained for Cambisols in the Selke catchment. Table 3 results show that stream flow in the model was most sensitive to the runoff recession coefficient in the uppermost soil layer (*rrcs1*) for the dominant soil type (red soil, *RCS* = 3.17). This highlights the significance of catchment-stream connectivity, because higher values of *rrcs1* indicate greater discharge from soils for a given soil water content. The model stream flow was also sensitive to the maximum percolation capacity (*mperc*) of red soil and maximum velocity in the stream channel (*rivvel*), indicating the effects of percolation and the characteristics of stream transmission on stream flow simulation. We note that parameter sensitivity varied by two orders of magnitude (see *RCS* in Table 3), whereby three of the ten hydrology parameters chosen for calibration exerted dominant roles on the model.

P transport modelling was found most sensitive to the exponent in the equation for calculating erosion caused by surface runoff (*sreroexp*, *RCS* = 666), indicating the controlling role of soil erosion on P mobilization. This is consistent with findings from field experiments by Chen (2013), who demonstrated that sediment erosion and transport by surface flow was the main mechanism leading to P export from sloping agricultural land in the subtropical monsoon area of the Three Gorges Reservoir catchment. The exponent (*freund2*) and coefficient (*freund1*) in the Freundlich equation (i.e., p_{FREX} and p_{FRCO} in equation 2), describing adsorption/desorption processes in red soil, have the second highest (*RCS* = 166) and third highest (*RCS* = 101) sensitivities, respectively. The mineralization rate (*minerfp*) for forest and the exponent in the

Freundlich equation (*freund2*) for paddy soil are also sensitive, with *RCS* values of 43 and 42, respectively. This is consistent with the findings from Bender et al. (2018), who demonstrated the important role of erosion processes on the transfer of PP, and the influence of adsorption/desorption on DP during storm events in a subtropical rural catchment in southern Brazil. Of the ten P-process parameters tested, three parameters (*sreroexp*, *freund2* and *freund1* for red soil) produced sensitivities that were orders of magnitude greater than other parameter sensitivities. Thus, it appears that P export in the HYPE model is dependent on the values of a relatively small number of parameters.

3.3 Discharge simulation

Figures 4 and 5 show the comparison between the simulated and observed daily discharge at the six gauging stations during calibration and validation periods. Table 5 provides a summary of corresponding calibration statistics in relation to discharge. Stream flow dynamics are well represented for both calibration and validation modes across all gauging stations, with *NSE* ranging between 0.73 and 0.92 (Table 5). During the second validation period (1 Jan 2009 - 31 Dec 2011), the model performance was lowest for the upstream station of Xiang Tun (i.e., *NSE* = 0.73), whereas the downstream stations (Hu Shan, Shi Zhen Jie) had *NSE* values of 0.91 and 0.92, respectively.

The timing of peak flows generated by heavy rainfall events in summer was mostly well captured; however, some underestimation of flood magnitudes was observed. Underestimation of peak flows has been reported in a number of other catchment modelling studies that adopt daily time steps (e.g., Jiang et al., 2014; Lam et al., 2012; Pathak et al., 2018; Rode et al., 2009). This discrepancy has been mainly attributed to limitations introduced by adopting daily time steps,

combined with measurement uncertainties associated with both rainfall and high stream flow rates. That is, peak flow rates may arise from processes occurring at sub-daily time steps that are not well captured by daily simulation. Also, the reliability of stream flow gauging is known to diminish for high flow events (Hamilton and Moore, 2012). Additionally, spatial and temporal variability of rainfall during peak events is often not well characterised when rainfall stations are relatively sparse, as is the case for the current study. Despite these challenges, the bias of model discharge rates is reasonably low for the period 1 Jan 1978 - 31 Dec 1986, with |*PBIAS*| ranging from 0.2 to 14.5% (Table 5).

Figure 4 near here

Figure 5 near here

Table 5. Statistic model performance (daily discharge) for the calibration period (1 Jan 1978 - 31 Dec 1982) and first validation period (1 Jan 1983 - 31 Dec 1986) at six discharge gauging stations (Wang Kou, San Du, Yin Shan, Xiang Tun, Hu Shan and Shi Zhen Jie); and for the second validation period (1 Jan 2009 - 31 Dec 2011) at three discharge gauging stations (Xiang Tun, Hu Shan, and Shi Zhen Jie). *PBIAS* has the unit of %, while other variables are unitless.

Station	**Upstream area (km^2)**	**Calibration**			**First validation period**		
		NSE	***RSR***	***PBIAS***	***NSE***	***RSR***	***PBIAS***
Wang Kou	581	0.86	0.37	-10.1	0.80	0.44	-8.6
San Du	1407	0.89	0.33	5.6	0.82	0.42	14.5
Yin Shan	471	0.88	0.35	-10.2	0.84	0.40	-6.9
Xiang Tun	3878	0.92	0.29	4.2	0.88	0.35	2.5
Hu Shan	6348	0.90	0.32	-0.4	0.87	0.36	-0.2
Shi Zhen Jie	8324	0.84	0.40	-5.1	0.87	0.36	-2.6
					Second validation period		
Xiang Tun	3878				0.73	0.52	-2.7
Hu Shan	6348				0.91	0.33	-3.0
Shi Zhen Jie	8324				0.92	0.34	-5.4

The Le An River catchment experiences significant temporal variability in rainfall patterns, and consequently, runoff totals. For example, average rainfall rates of 1515 mm/yr and 1783 mm/yr led to mean runoff values of 921 mm/yr and 1103 mm/yr during the periods 1978-1986 and 2009-2011, respectively. Annual runoff totals varied by almost two-fold during 2009-2011, with values of 860 mm, 1622 mm and 827 mm obtained for 2009, 2010 and 2011, respectively. At the station Shi Zhen Jie, an extreme storm event (rainfall amount 217 mm on 16 Jun 2011) led to peak discharge of 7290 m^3/s with average recurrence interval of 44 years. Stream flow dynamics were well captured at all three stations (Xiang Tun, Hu Shan, Shi Zhen Jie) over the three-year period 2009-2011, with $NSE \geq 0.73$ and $|PBIAS| \leq 5.4\%$ (Figure 5, Table 5).

PBIAS values in Table 5 show that spatial variations in bias are apparent in the HYPE results, whereby the largest underestimations in stream flow were obtained at upstream sites (e.g., Wang Kou, Yin Shan). Other HYPE modelling studies (of temperate catchments) also led to greater bias in stations at higher elevations than those at lower elevations (e.g., Jiang et al., 2014; Strömqvist et al., 2012). This is most likely because rainfall over mountainous regions was under-measured due to the influence of topography, which causes variations of rainfall over distances smaller than the spacing between meteorological stations (Chaubey et al., 1999). Higher elevations likely receive greater rainfall (than that estimated from interpolation between widely spaced meteorological stations), thereby leading to underestimation in stream flow at upstream stations. In general, the model performance in terms of discharge simulation is considered robust across different tempo-spatial domains and classified as "good" to "very good" based on the model evaluation guidelines specified by Moriasi et al. (2007). We consider that this indicates reasonable representation of catchment-scale hydrological processes.

3.4 P export simulation

The simulated and observed stream TP concentrations from stations WQ1-WQ6 are shown as a scattergram in Figure 6. Underestimation of high TP concentrations (red dots in Figure 6) primarily occurred: (i) during low-flow conditions (August-December 2010) at the downstream site WQ6, and (ii) during a storm event (August 2011) in upstream sites (WQ2, WQ4). The underestimation of TP concentrations at the downstream site is likely a consequence of input errors/uncertainty in point sources in terms of P concentrations and/or volume of sewage/industry effluent, which pose more significant effects on stream P concentrations during low-flow conditions due to limited dilution capacity. The underestimation of TP concentrations during the storm event in upstream areas is likely related to the under-prediction of surface runoff during the

storm event (Figure 5), leading to underestimation in soil erosion, for which P export is sensitive. Moreover, uncertainty in the simulation of primary production (i.e., biological uptake) could also be an important reason for the bias, as stream P concentration is sensitive to the primary production parameter (*wprod*, *RCS* = 10.7). In-stream retention (e.g., biological uptake, denitrification) of dissolved nutrients is affected by temperature, light conditions, flow residence time, stream flow variability and catchment scale (Minaudo et al., 2019; Ye et al., 2012). The underestimation of TP concentrations greater than 0.2 mg/L (red dots in Figure 6) may imply that a process/source of P is not being modelled. The bias in model-estimated TP concentrations was small, with overestimation less than 1% (*PBIAS* = 0.97%). Despite under-estimation of high TP values, the *RSR* value of 0.68 falls in the "satisfactory" category ($0.60 < RSR \leq 0.70$), according to guidelines for the evaluation of watershed model performance proposed by Moriasi et al. (2007).

Figure 6 near here

Figure 7 presents the comparison of simulated and observed average monthly TP loads at the catchment outlet (station Shi Zhen Jie) during 1 Jan 2009 - 31 Dec 2011. HYPE captures reasonable well the intra-annual variations in TP loads (i.e., *NSE* = 0.55, *PBIAS* = 8.34%). TP loads during March-August are highest, coinciding with the highest rates of rainfall-runoff, and the most active period of agricultural activity. Lower TP loads occur during low-flow conditions (September-February) even though stream TP concentrations were highest during this period. Thus, intra-annual variations in TP loads appear contingent primarily on hydrological variability. The simulated and observed average annual TP loads are 1287 t/yr and 1187 t/yr, respectively, indicating model overestimation by 8.5%. On average, TP loads during March-August accounted for 74.3% of the annual TP load, with corresponding total runoff during this period equal to 82.7% of annual runoff. Table 6 lists the simulated and observed TP, DP and PP yields from the

upstream areas (above station WQ3), lowland plains region (areas between WQ3 and WQ6), and whole catchment for 2016. Model performance in relation to TP yields for all three sites are classified as "satisfactory" (PBIAS<±70%), while representation of PP yields at upstream areas, and DP yields at lowland plains region and whole catchment are classified as "unsatisfactory" according to Moriasi et al. (2007), due to substaintial overestimation.

Figure 7 near here

Table 6. Simulated (Sim) and observed (Obs) TP, DP and PP yields (kg/ha) for 2016 from the upstream areas (above station WQ3), lowland plains region (areas between WQ3 and WQ6), and whole catchment showing different physiographic characteristics (area, elevation, slope and land use).

Site	Area (km^2)	Average elevation (m)	Average slope (%)	Land use (%)			TP (kg/ha)		DP (kg/ha)		PP (kg/ha)	
				Forest	Arable land	Urban area	Sim	Obs	Sim	Obs	Sim	Obs
Upstream areas	3878	220	20.4	86.8	9.7	0.9	0.88	0.71	0.18	0.43	0.48	0.26
Lowland plains region	4435	132	12.9	63.8	27.2	2.2	4.69	3.19	2.15	0.87	2.55	2.54
Whole catchment	8324	176	16.6	74.5	19.0	1.6	2.91	2.03	1.33	0.66	1.58	1.47

A significant percentage of the annual TP export is released during short periods of high rainfall. For example, 16.2% of the total TP load for 2009 was exported during an 11-day period (20-30 April 2009) with corresponding total rainfall 60.4 mm, or 4.3% of the 2009 rainfall. Similarly, 15.2% of the total TP load during 2010 occured during a 10-day period (9-18 July), when the catchment received rainfall totalling 237.5 mm, equal to 9.7% of the 2010 rainfall. 46.7% of the TP load of 2011 was exported during an 8-day period (15-22 June), when 380.1 mm rainfall occured (25.2% of the 2011 total). The high contribution of storm flow events during April-July to annual TP loads, as described here, are likely the consequence of: (i) fertilisation practices carried out in the catchment (which occur mainly in spring and summer), and (ii) ability of heavy rainfall to flush both particulate and dissolved P from soils and transport P to streams (Minaudo et al., 2019). This supports the findings from previous P export studies. For example, Rodríguez-Blanco et al. (2013) reported that high-rainfall events contributed to 68% of P exported over a 5-year period in the Corberia catchment, NW Spain. Pionke et al. (1996) found that P export (DP, PP) was dominated by storm periods from an agricultural hill-land watershed in Pennsylvania. Sharpley et al. (2008) demonstrated that release of P from soil stores increases with storm size in the Susquehanna River catchment. Udawatta et al. (2004) determined that the five largest runoff events out of a total of 66 events over seven years accounted for 27% of the TP loads from three adjacent agricultural watersheds in the claypan region of the northeastern Missouri. Fang et al. (2015) illustrated the dominant role of storm events on sediment and associate PP loss in a subtropical watershed in China, who attributed 95% of the sediment load to 30 runoff events within a 7 year period. TP yields during 2009-2011 and 2016 had the ranges of 0.24-0.88 kg/ha/yr and 4.31-4.69 kg/ha/yr for the upstream areas above station Xiang Tun and downstream areas (i.e., plains region between stations Xiang Tun and Shi Zhen Jie), respectively.

4. Discussion

Through evaluation of model performance on stream flow and TP loads (Figures 4-7, Tables 5-6), HYPE was found capable to represent reasonably well temporal variability of runoff and P export under different climatic conditions. The average proportions of DP in TP during 2009-2011 for stations WQ1 to WQ6 and 2016 (stations WQ3, WQ6) ranged from 20.3 to 58.6%. The export coefficient (i.e., annual export rate) of TP and PP obtained from the current study are mostly higher than those of previous studies that consider similar climate, hydrology and land use characteristics (e.g., Song et al., 2014; Udawatta et al., 2004). For example, the average annual export rates of TP and DP range from 0.24 to 4.69 kg/ha/yr and from 0.18 to 2.15 kg/ha/yr, respectively across different sites (notwithstanding the overestimation of DP yields at the lowland plains region). Udawatta et al. (2004) obtained TP loads of 0.29 to 3.59 kg/ha/yr for the claypan region of Missouri (USA) based on intensive sampling during runoff events at three small watersheds (areas 1.65-4.44 ha). Xi (2014) estimated TP loads of 0.37 to 1.22 kg/ha/yr through P transport modelling with AnnAGNPS at a subtropical monsoon catchment (area 47.85 km^2) in southeastern China. Song et al. (2014) obtained the TP loads of 0.02 kg/ha/month and 0.06 kg/ha/month based on monitoring of two subtropical agricultural catchments in the hilly red soil covered region of China with respective proportions of SP in TP of 47.1% and 37.5%.

The significant contribution of storm flow events to annual TP loads, obtained from the current P export simulation, is consistent with findings from other storm events-based P transport studies (e.g., Fang et al., 2015; Pionke et al., 1996; Sharpley et al., 2008; Udawatta et al., 2004). Bender et al. (2018) suggested that efforts towards adopting erosion-reducing practices can contribute to reduction of sediment loss and P transfer to water cources, based on assessment of P dynamics in a subtropical rural catchment during storm events in southern Brazil. Other effective measures to

reduce diffuse agricultural P export include optimizing fertiliser addition in terms of application timing and rate, minimizing soil disturbance at harvested sites by reducing tillage and filtration via buffer/raparian zones (Santos et al., 2015; Sharpley et al., 2000). Our study showed that the use of catchment water quality modelling can strongly constrain estimates of P losses from anthropogenic impacted landscapes in China but that empirical research is still needed to provide a better basis for calibrating models and deriving export coefficients (see also Ongley et al. 2010).

The characteristics of model mismatch (simulated versus observed P loads) provide some insight into areas for improving model accuracy. Firstly, the reliability of nutrient sources needs to be improved, including diffuse agricultural sources and point sources from sewage treatment works, as the errors/uncertainty in nutrient inputs contribute greatly to the mismatch in simulation of stream P concentrations (Figure 6). Secondly, it is necessary to increase the stream P sampling frequency, especially during storm flow events. In the Le An River catchment, the monthly water quality sampling campaign does not allow for adequate characterisation of flow conditions, especially storm flow events. This may lead to uncertainty in parameter calibration and subsequently bias in simulation of stream TP concentrations and TP loads, considering the major contribution of storm flow events to annual total TP loads. For instance, Rodríguez-Blanco et al. (2013) related around 67% of the P export to precipitation events from a mixed land use catchment in Galicia (NW Spain). Thirdly, whereas studies of P export such as Kronvang et al. (1997) and Wu et al. (2018) include observations of suspended sediment, the current study is limited by a lack of suspended sediment measurements. Hence, incorporating suspended sediment concentrations into simulation and calibration of HYPE parameters for sediment detachment and transport would assist in model accuracy by constraining PP, because P export

simulation is most sensitive to surface runoff erosion (*sreroexp*, *RCS* = 666). The observed suspended sediment concentrations should correlate with PP concentrations (Sandstroem et al., 2020). If they do not, then it would indicate a non-upland source of PP, such as in-stream remobilizing of fine river-bed sediments (Minaudo et al., 2018). Finally, an investigation of the impacts of various uncertainty sources (e.g., input data, model structure and calibration) on model simulation of hydrology and P export could assist in diagnosis of model deficit (Hollaway et al., 2018). Furthermore, it could guide model development and risk-based decision making on catchment management measures to tackle the problem of P pollution (Jiang et al., 2019; Wellen et al., 2015). This study implies that practices to control soil erosion, optimize agriculture management (especially fertiliser application), and improve waste water collection and treatment would be essential to reduce P export and improve water quality in subtropical regions, like Le An Le An River catchment.

5. Conclusions

Hydrological and phosphorus (P) export modeling of a subtropical monsoon catchment (Le An River catchment) was undertaken using HYPE, a semi-distributed process-based model. Model calibration produced a reasonable match between simulated and measured stream flow, total P (TP) and dissolved P (DP), although discrepancies in stream P fluxes occurred. The parameters shown to be have the high sensitivity for TP and DP fluxes during high-flow and low-flow conditions were *freund2* and *freund3* that describe adsorption/desorption process of soil P for red soil and paddy soil. The high TP loads (2.91 kg/ha/yr) in the Le An River catchment are attributed to higher rates of point sources input in the form of human and industrial effluent, as compared to the Tuo Jia and Zhong Tian River catchments, where point-source inputs are lower (e.g., Song et al., 2014; Xi, 2014).

Stream total P (TP) and dissolved P (DP) concentrations showed negative relationships with river flow rates in the lowland plains region, which is more urbanised and has a higher percentage of arable land relative to the forested upstream areas. This indicates that stream P concentrations in that area are dominated by dilution effects, whereby P transport capacity is low during low-flow conditions. In forested upland areas, stream TP and DP concentrations showed near chemostatic behaviour (i.e., the variations in TP and DP concentrations are low).

Sensitivity analysis indicated that P export is most sensitive to soil erosion from surface runoff and adsorption/desorption of soil P. The importance of soil erosion was also reflected in intra-annual patterns of TP loads at the catchment outlet, whereby most of the TP load occurring in each year was attributable to high-rainfall periods (March-August) for both upland and lowland areas, when intensive agricultural activity appears to mobilize P through erosion and high PP fluxes. It implies that in anthropogenically impacted subtropical catchments like the Le An River catchment, measures to decrease TP load, which are particularly important for receiving water bodies (e.g., Poyang Lake), should focus on reducing soil erosion and P mobilization from overland flow, whereas reduction of the time-averaged TP concentrations, which is more relevant for riverine ecosystems, should emphasis on point sources input.

Acknowledgments

This work is supported by the National Natural Science Foundation of China (grant no. 41877487, 41501531), the Open Research Fund of State Key Laboratory of Simulation and Regulation of Water Cycle in River Basin, the China Institute of Water Resources and Hydropower Research (grant no. IWHR-SKL-201710), the Sino-German Cooperation Group

(GZ1447), and the Science and Technology Project funded by Jiangxi Provincial Water Conservancy Bureau (grant no. 201820YBKT02).

References

Allen, B.L., Mallarino, A.R., 2008. Effect of liquid swine manure rate, incorporation, and timing of rainfall on phosphorus loss with surface runoff. J. Environ. Qual., 37, 125-137.

Arnold, C.L., Gibbons, C.J., 1996. Impervious surface coverage: the emergence of a key environmental indicator. J. Am. Plann. Assoc., 62, 243-258.

Arnold, J.G., Srinivasan, R., Muttiah, R.S., Williams, J.R., 1998. Large area hydrological modeling and assessment part I: model development. J. Am. Water Resour. As., 34, 73-89.

Bender, M.A., dos Santos, D.R., Tiecher, T., Minella, J.P.G., de Barros, C.A.P., Ramon, R., 2018. Phosphorus dynamics during storm events in a subtropical rural catchment in southern Brazil. Agric. Ecosyst. Environ., 261, 93-102.

Beven K.J., Binley A.M., 1992. The future of distributed models: model calibration and predictive uncertainty. Hydrol. Process., 6, 279-298.

Bingner, R.L., Theurer, F.D., Yuan, Y., 2012. AnnAGNPS Technical Processes. USDA – ARS National Sedimentation Laboratory, http://www.ars.usda.gov/Research/docs.htm?docid=5199.

Bitschofsky, F., Nausch, M., 2019. Spatial and seasonal variations in phosphorus speciation along a river in a lowland catchment (Warnow, Germany). Sci. Total Environ., 657, 671-685.

Brendel, C.E., Soupir, M.L., Long, L.A.M., Helmers, M.J., Ikenberry, C.D., Kaleita, A.L., 2019. Catchment-scale Phosphorus Export through Surface and Drainage Pathways. J. Environ. Qual., 48 (1), 117-126.

Cao, D., Cao, W., Fang, J., Cai, L., 2014. Nitrogen and phosphorus losses from agricultural systems in China: a meta-analysis. Mar. Pollut. Bull., 85 (2), 727-732.

Carpenter, S.R., Caraco, N.F., Correll, D.L., Howarth, R.W., Sharpley, A.N., Smith, V.H., 1998. Nonpoint pollution of surface waters with phosphorus and nitrogen. Ecol. Appl., 8 (3), 559-568.

Chaubey, I., Haan, C.T., Grunwald, S., Salisbury, J.M., 1999. Uncertainty in the model parameters due to spatial variability of rainfall. J. Hydrol., 220, 48-61.

Chen, J., Lu, J., 2014. Effects of land use, topography and socio-economic factors on river water quality in a mountainous watershed with intensive agricultural production in East China. PLoS One, 9 (8), e102714.

Chen, L., 2013. Research on nitrogen and phosphorus loss characteristics in sloping arable land in Xiangxi Bay. China Three Gorges University, Masters Dissertation.

Conley, D.J., Paerl, H.W., Howarth, R.W., Boesch, D.F., Seitzinger, S.P., Havens, K.E., Lancelot, C., Likens, G.E., 2009. Ecology controlling eutrophication: nitrogen and phosphorus. Science, 323, 1014-1015.

Correll, D.L., 1999. Phosphorus: A Rate Limiting Nutrient in Surface Waters. Poultr. Sci., 78, 674-682.

Cuo, L., Giambelluca, T.W., Ziegler, A.D., 2011. Lumped parameter sensitivity analysis of a distributed hydrological model within tropical and temperate catchments. Hydrol. Process., 25, 2405-2421.

De Borba, B.M., Jack, R.F., Rohrer, J.S., Wirt, J., Wang, D., 2014. Simultaneous determination of total nitrogen and total phosphorus in environmental waters using alkaline persulfate digestion and ion chromatography. J. Chromatogr. A, 1369, 131-137.

Deng, X.Z., Zhao, Y.H., Wu, F., Lin, Y.Z., Lu, Q., Dai, J., 2011. Analysis of the trade-off between economic growth and the reduction of nitrogen and phosphorus emissions in the Poyang Lake Watershed, China. Ecol. Modell., 222, 330-336.

Dong, Y.Y., 2013. Contingent Valuation of Yangtze Finless Porpoises in Poyang Lake, China. Springer Netherlands, Doi: 10.1007/978-94-007-2765-6.

Doherty, J., 2016. PEST User Manual. Part I and II. Watermark Numerical Computing, Brisbane, Australia.

Donigian, A.S., Bicknell, B.R., Imhoff, J.C., 1995. Hydrological simulation program - Fortran (HSPF). In Singh, V.P. (Eds.), Computer Models of Watershed Hydrology, Water Resources Publications, Highlands Ranch, Colorado, USA, pp. 395-442.

Duan, S., Liang, T., Zhang, S., Wang, L.J., Zhang, X.M., Chen, X.B., 2008. Seasonal changes in nitrogen and phosphorus transport in the lower Changjiang River before the construction of the Three Gorges Dam. Estuarine Coastal Shelf Sci., 79 (2), 239-250.

Dupas, R., Mellander, P.-E., Chantal-Odoux, C., Fovet, P., McAleer, E.B., McDonald, N.T., Shore, M., Jordan, P., 2017. The role of mobilisation and delivery processes on contrasting dissolved nitrogen and phosphorus exports in groundwater fed catchments. Sci. Total Environ., 599-600, 1275-1287.

Duval, T.P., 2018. Effect of residential development on stream phosphorus dynamics in headwater suburbanizing watersheds of southern Ontario, Canada. Sci. Total Environ., 637-638, 1241-1251.

Edwards, A.C., Chambers, P.A., 2002. Quantifying nutrient limiting conditions in temperate river systems. In Haygarth, P.M., Jarvis, S.C. (Eds.): Agriculture, Hydrology and Water Quality, CAB International, Wallingford, USA, pp. 477-493.

Edwards, A.C., Twist, H., Codd, G.A., 2000. Assessing the impact of terrestrially derived phosphorus on flowing water systems. J. Environ. Qual., 29, 117-124.

EEA. http://www.eea.europa.eu/data-and-maps/indicators/nitrogen-and-phosphorus-inrivers, 2010.

Fang, N.F., Shi, Z.H., Chen, F.X., Zhang, H.Y., Wang, Y.X., 2015. Discharge and suspended sediment patterns in a small mountainous watershed with widely distributed rock fragments, J. Hydrol., 528, 238-248.

Freni, G., Mannina, G., 2010. Bayesian approach for uncertainty quantification in water quality modelling: the influence of prior distribution. J. Hydrol., 392 (1-2), 31-39.

Fischer, T., Fischer, T., Menz, C., Su, B., Scholten, T., 2013. Simulated and projected climate extremes in the Zhujiang River Basin, South China, using the regional climate model COSMO-CLM. Int. J. Climatol., 33 (14), 2988-3001.

Gao, Y., Hao, Z., Yang, T.T., He, N.P., Wen, X.F., Yu, G.R., 2017. Effects of atmospheric reactive phosphorus deposition on phosphorus transport in a subtropical watershed: A Chinese case study. Environ. Pollut., 226, 69-78.

Garnache, C., Swinton, S.M., Herriges, J.A., Lupi, F., Stevenson, R.J., 2016. Solving the Phosphorus Pollution Puzzle: Synthesis and Directions for Future Research. Am. J. Agr. Econ., 98 (5), 1334-1359.

Gurung, D.P., Githinji, L.J.M., Ankumah, R.O., 2013. Assessing the Nitrogen and Phosphorus Loading in the Alabama (USA) River Basin Using PLOAD Model. Air Soil Water Res., 6, 23-36.

Godsey, S.E., Kirchner, J.W., Clow, D.W., 2009. Concentration-discharge relationships reflect chemostatic characteristics of US catchments. Hydrol. Process., 23 (13), 1844-1864.

Hamilton, A.S., Moore, R.D., 2012. Quantifying uncertainty in streamflow records, Can. Water Resour. J., 37, 13-21.

Hansen, N.C., Daniel, T.C., Sharpley, A.N., Lemunyon, J.L., 2002. The fate and transport of phosphorus in agricultural systems. J. Soil Water Conserv., 57 (6), 408-417.

Hollaway, M.J., Beven, K.J., Benskin, C.McW.H., Collins, A.L., Evans, R., Falloon, P.D., Forber, K.J., Hiscock, K.M., Kahana, R., Macleod, C.J.A., Ockenden, M.C., Villamizar, M.L., Wearing, C., Withers, P.J.A., Zhou, J.G., Barber, N.J., Haygarth, P.M., 2018. The challenges of modelling phosphorus in a headwater catchment: Applying a 'limits of acceptability' uncertainty framework to a water quality model. J. Hydrol., 558, 607-624.

Hu, C.H., 2010. The Water Environmental Characteristic and Its Evolutionary Trends of Poyang Lake. Nanchang University, PhD Dissertation.

Hunsaker, C.T., Johnson, D.W., 2017. Concentration-discharge relationships in headwater streams of the Sierra Nevada, California. Water Resour. Res., 53 (9), 7869-7884.

Jackson-Blake, L.A., Dunn, S.M., Helliwell, R.C., Skeffington, R.A., Stutter, M.I., Wade, A.J., 2015. How well can we model stream phosphorus concentrations in agricultural catchments? Environ. Modell. Software., 64, 31-46.

Jiang, S.Y., Zhang, Q., Werner, A.D., Wellen, C., Jomaa, S., Zhu, Q.D., Büttner, O., Meon, G., Rode, M., 2019. Effects of stream nitrate data frequency on watershed model performance and prediction uncertainty. J. Hydrol., 569, 22-36.

Jiang, S.Y., Jomaa, S., Buettner, O., Meon, G., Rode, M., 2015. Multi-site identification of a distributed hydrological nitrogen model using Bayesian uncertainty analysis. J. Hydrol., 529, 940-950.

Jiang, S.Y., Jomaa, S., Rode, M., 2014. Modelling inorganic nitrogen emissions at a nested mesoscale catchment in central Germany. Ecohydrology, 7 (5), 1345-1362.

Jiang, S.Y., Rode, M., 2012. Modeling water flow and nutrient losses (Nitrogen, Phosphorus) at a nested mesoscale catchment, Germany. International Congress on Environmental Modelling and Software(iEMSs), Managing Resources of a Limited Planet, Sixth Biennial Meeting, Leipzig, Germany.

Jiang, Y., Xie, Z.L., Zhang, H., Xie, H.Q., Cao, Y., 2017. Effects of land use types on dissolved trace metal concentrations in the Le'an River Basin, China. Environ. Monit. Assess., 189 (12), Art. no. 633.

Jiao, J., Ellis, E.C., Yesilonis, I., Wu, J., Wang, H., Li, H., Yang L., 2010. Distributions of soil phosphorus in China's densely populated village landscapes. J. Soil Sediment, 10, 461-472.

Jin, L., Whitehead, P.G., Rodda, H., Macadam, T., Sarkar, S., 2018. Simulating climate change and socio-economic change impacts on flows and water quality in the Mahanadi River system, India. Sci. Total Environ., 637-638, 907-917.

Jomaa, S., Jiang, S.Y., Thraen, D., Rode, M., 2016. Modelling the effect of different agricultural practices on stream nitrogen load in central Germany. Energy, Sustain. Soc., 6 (11), 1-16.

Lai, G., Yu, G., Gui, F., 2006. Preliminary study on assessment of nutrient transport in the Taihu Basin based on SWAT modeling. Sci. China Ser. D, 49 (1), 135-145.

Lazzarotto, P., Prasuhn, V., Butscher, E., Crespi, C., Fluehler, H., Stamm, C., 2005. Phosphorus export dynamics from two Swiss grassland catchments. J. Hydrol., 304 (1-4), 139-150.

Li, X., Hu, Q., 2019. Spatiotemporal changes in extreme precipitation and its dependence on topography over the Poyang Lake Basin, China. Adv. Meteorol., 2019, Art. no. 1253932.

Li, Z.F., Luo, C., Jiang, K.X., Wan, R.R., Li, H.P., 2017. Comprehensive performance evaluation for hydrological and nutrients simulation using the Hydrological Simulation Program-Fortran in a mesoscale monsoon watershed, China. Int. J. Environ. Res. Public Health., 14 (12), Art. no. 1599.

Li, S., Gu, S., Liu, W., Han, H., Zhang, Q., 2008. Water quality in relation to land use and land cover in the upper Han River Basin, China. Catena, 75 (2), 216-222.

Li, Z.F., Luo, C., Xi, Q., Li, H.P., Pan, J.J., Zhou, Q.S., Xiong, Z.Q., 2015. Assessment of the AnnAGNPS model in simulating runoff and nutrients in a typical small watershed in the Taihu Lake basin, China. Catena, 133, 349-361.

Liu, Q.C., Yu, C., Zhang, J., Chen, X., Ge, G., Wu, L., 2013. Water quality variations in Poyang Lake. Journal of Agro-Environment Science, 32 (6), 1232-1237 (in Chinese).

Lu, S.Y., Zhang, P., Pan, C.R., Peng, S.C., Liu, X.H., 2017. Agricultural non-point source pollution discharge characteristic and its control measures of Dongting Lake. China Environmental Science, 37 (6), 2278-2286 (in Chinese).

Kaye, J.P., Groffman, P.M., Grimm, N.B., Baker, L.A., Pouyat, R.V., 2006. A distinct urban biogeochemistry? Trends Ecol. Evol., 21 (4), 192-199.

Kim, J.S., Oh, S.Y., Oh, K.Y., 2006. Nutrient runoff from a Korean rice paddy watershed during multiple storm events in the growing season. J. Hydrol., 327 (1-2), 128-139.

Kim, K., Kim, B., Eum, J., Seo, B., Shopre, C.L., Peiffer, S., 2018. Impacts of Land Use Change and Summer Monsoon on Nutrients and Sediment Exports from an Agricultural Catchment. Water, 10 (5), Art. no. 544.

Kronvang, B., Laubel, A., Grant, R., 1997. Suspended sediemnt and particulate phosphorus transport and delivery pathways in an arbale catchment, Gelbæk Stream, Denmark. Hydrol. Process., 11 (6), 627-642.

Lagzdins, A., Jansons, V., Sudars, R., Abramenko, K., 2012. Scale issues for assessment of nutrient leaching from agricultural land in Latvia. Hydrol. Res., 43, 383-399.

Lam, Q.D., Schmalz, B., Fohrer, N., 2012. Assessing the spatial and temporal variations of water quality in lowland areas, Northern Germany. J. Hydrol., 438-439, 137-147.

Lindström, G., Pers, C., Rosberg, J., Strömqvist, J., Arheimer, B., 2010. Development and testing of the HYPE (Hydrological Predictions for the Environment) water quality model for different spatial scales. Hydrol. Res., 41 (3-4), 295-319.

McDowell, R.W., Biggs, B.J.F., Sharpley, A.N., Nguyen, L., 2004. Connecting phosphorus loss from agricultural landscapes to surface water quality. Chem. Ecol., 20, 1-40.

Minaudo, C., Dupas, R., Gascuel-Odoux, C., Roubeix, V., Danis, P.-A., Moatar, F., 2019. Seasonal and event-based concentration-discharge relationships to identify catchment controls on nutrient export regimes. Adv. Water Resour., 131, 103379.

Moore, C.M., Mills, M.M., Langlois, R., Milne, A., Achterberg, E.P., Roche, J.L., Geider, R.J., 2008. Relative influence of nitrogen and phosphorus availability on phytoplankton physiology and productivity in the oligotrophic sub-tropical North Atlantic Ocean. Limnol. Oceanogr., 53 (1), 291-305.

Morgan, R.P.C., 2001. A simple approach to soil loss prediction: a revised Morgan-Morgan-Finney model. Catena, 44, 305-322.

Moriasi, D.N., Arnold, J.G., Liew, M.W.V., Bingner, R.L., Harmel, R.D., Veith, T.L., 2007. Model evaluation guidelines for systematic quantification of accuracy in watershed simulations. Trans. ASABE, 50, 885-900.

Neff, R., Chang, H., Knight, C.G., Najjar, R.G., Yarnal, B., Walker, H.A., 2000. Impact of climate variation and change on Mid-Atlantic Region hydrology and water resources. Clim. Res., 14 (3), 207-218.

Ongley, E.D., Zhang, X.L., Tao, Y., 2010. Current status of agricultural and rural non-point source Pollution assessment in China. Environ. Pollut., 158 (5), 1159-1168.

O'Neal, M.R., Nearing, M.A., Vining, R.C., Southworth, J., Pfeifer, R.A., 2005. Climate change impacts on soil erosion in Midwest United States with changes in crop management. Catena, 61, 165-184.

Palmer-Felgate, E.J., Mortimer, R.J.G., Krom, M.D., Jarvie, H.P., 2010. Impact of point-source pollution on phosphorus and nitrogen cycling in stream-bed sediments. Environ. Sci. Technol., 44, 908-914.

Panagopoulos, Y., Makropoulos, C., Baltas, E., Mimikou, M., 2011. SWAT parameterization for the identification of critical diffuse pollution source areas under data limitations. Ecol. Modell., 222, 3500-3512.

Pathak, D., Whitehead, P.G., Futter, M.N., Sinha, R., 2018. Water quality assessment and catchment-scale nutrient flux modelling in the Ramganga River Basin in north India: An application of INCA model. Sci. Total Environ., 631-632, 201-215.

Pionke, H.B., Gburek, W.J., Sharpley, A.N., Schnabel, R.R., 1996. Flow and nutrient patterns for an agricultural hill-land watershed. Water Resour. Res., 32, 1795-1804.

Rode, M., Klauer, B., Petry, D., Volk, M., Wenk, G., Wagenschein, D., 2008. Integrated nutrient transport modelling with respect to the implementation of the European WFD: The Weiße Elster Case Study, Germany. Water SA, 34, 490-496.

Rode, M., Thiel, E., Franko, U., Wenk, G., Hesser, F., 2009. Impact of selected agricultural management options on the reduction of nitrogen loads in three representative meso scale catchments in Central Germany. Sci. Total Environ., 407, 3459-3472.

Rodríguez-Blanco, M.L., Taboada-Castro, M.M., Taboada-Castro, M.T., 2013. Phosphorus transport into a stream draining from a mixed land use catchment in Galicia (NW Spain): Significance of runoff events. J. Hydrol., 481, 12-21.

Sandstroem, S., Futter, M.N., Kyllmar, K., Bishop, K., O'Connell, D.W., Djodjic, F., 2020. Particulate phosphorus and suspended solids losses from small agricultural catchments: Links to stream and catchment characteristics. Sci. Total Environ., 711, 134616.

Santos, R.M.B., Sanches Fernandes, L.F., Pereira, M.G., Cortes, R.M.V., Pacheco, F.A.L., 2015. A framework model for investigating the export of phosphorus to surface waters in forested watersheds: Implications to management. Sci. Total Environ., 536, 295-305.

Schoumans, O.F., Chardon, W.J., Bechmann, M.E., Gascuel-Odoux, C., Hofman, G., Kronvang, B., Rubaek, G.H., Ulen, B., Dorioz, J.M., 2014. Mitigation options to reduce phosphorus losses from the agricultural sector and improve surface water quality: a review. Sci. Total Environ., 468-469, 1255-1266.

Schwarz, G.E., Hoos, A.B., Alexander, R.B., Smith, R.A., 2006. The SPARROW Surface Water-Quality Model—Theory, Applications and User Documentation, U.S. Geological Survey Techniques and Methods, Section 3, 6-B3, ISSN: 2328-7055, https://pubs.er.usgs.gov/publication/tm6B3.

Seitzinger, S.P., Harrison, J.A., Dumont, E., Arthur, H.W., Bouwman, A.F., 2005. Sources and delivery of carbon, nitrogen, and phosphorus to the coastal zone: An overview of Global Nutrient Export from Watersheds (NEWS) models and their application. Global Biogeochem. Cycles, 19 (4), Art. no. GB4S01.

Serpa, D., Nunes, J.P., Keizer, J.J., Abrantes, N., 2017. Impacts of climate and land use changes on the water quality of a small Mediterranean catchment with intensive viticulture. Environ. Pollut., 224, 454-465.

Sharpley, A., Foy, B., Withers, P., 2000. Practical and innovative measures for the control of agricultural phosphorus losses to water: An overview. J. Environ. Qual., 29 (1), 1-9.

Sharpley, A.N., Kleinman, P.J., Heathwaite, A.L., Gburek, W.J., Folmar, G.J., Schmidt, J.P., 2008. Phosphorus loss from an agricultural watershed as a function of storm size. J. Environ. Qual., 37, 362-368.

Sharpley, A.N., Kleinman, P.J.A., McDowell, R.W., Gitau, M., Bryant, R.B., 2002. Modelling phosphorus transport in agricultural watersheds: Processes and possibilities. J. Soil Water Conserv., 57, 425-439.

Shigaki, F., Sharpley, A.N., Prochnow, L.I., 2006. Source-related transport in surface runoff. J. Environ. Qual., 35 (6), 2229-2235.

Smith, V.H., Tilman, G.D., Nekola, J.C., 1999. Eutrophication: impacts of excess nutrient inputs on freshwater, marine, and terrestrial ecosystems. Environ. Pollut., 100, 179-196.

Song, L.F., Wang, Y., Wu, J.S., Li, Y., Li, Y.Y., Meng, C., Li, H., Zhang, M.Y., 2014. Impact of rice agriculture on nitrogen and phosphorus exports in streams in hilly red soil earth region of central subtropics. Environmental Science, 35 (1), 150-156 (in Chinese).

Strömqvist, J., Arheimer, B., Dahné, J., Donnelly, C., Lindström, G., 2012. Water and nutrient predictions in ungauged basins: Set-up and evaluation of a model at the national scale. Hydrol. Sci. J., 57, 229-247.

Sun, Z.B., Chen, Z.J., Liao, X.Y., Wang, H.M., 2011. Characteristics of agricultural non-point source nitrogen and phosphorus losses in a typical small watershed in Three Georges Reservoir Area. Chinese Journal of Ecology, 30 (8), 1720-1725 (in Chinese).

Tang, J.-L., Zhang, B., Gao, C., Zepp, H., 2008. Hydrological pathway and source area of nutrient losses identified by a multi-scale monitoring in an agricultural catchment. Catena, 72, 374-385.

Trindade, P.B.C.B., Coutinho, L.F.N., Caiado, M.A., Heatwole, C., 2010. Evaluation of nutrient modelling by SWAT under tropical conditions. 21st Century Watershed Technology:

Improving Water Quality and Environment CD-Rom Proceedings, 21-24 February 2010, Universidad EARTH, Costa Rica.

Udawatta, R.P., Motavalli, P.P., Garrett, H.E, 2004. Phosphorus loss and runoff characteristics in three adjacent agricultural watersheds with claypan soils. J. Environ. Qual., 33, 1709-1719.

Wade, A.J., Whitehead, P.G., Butterfield, D., 2002. The Integrated Catchments model of Phosphorus dynamics (INCA-P), a new approach for multiple source assessment in heterogeneous river systems: model structure and equations. Hydrol. Earth Syst. Sci., 6, 583-606.

Wang, M., Wang, Y., Li, Y., Liu, X., Liu, J., Wu, J., 2020. Natural and anthropogenic determinants for riverine phosphorus concentration and loading variability in subtropical agricultural catchments. Agric. Ecosyst. Environ., 287, 106713.

Wang, M.L., Zhou, W.B., Hu, C.H., 2008. Status of nitrogen and phosphorus in waters of Lake Poyang Basin. J. Lake Sci., 20 (3), 334-338.

Wang, Q.X., Xiao, Q.A., Liu, C., Wang, K.L., Ye, M., Lei, A., Song, X.F., Kohata, K., 2012. Effect of reforestation on nitrogen and phosphorus dynamics in the catchment ecosystems of subtropical China: the example of the Hanjiang River basin. J. Sci. Food Agric., 92 (5), 1119-1129.

Wang, Y., Li, Y., Liu, F., Li, Y.Y., Song, L.F., Li, H., Meng, C., Wu, J.S., 2014. Linking rice agriculture to nutrient chemical composition, concentration and mass flux in catchment streams in subtropical central China. Agric. Ecosyst. Environ., 184, 9-20.

Wang, Y.Y., Jia, Y.F., Guan, L., Lu, C., Lei, G.C., Wen, L., Liu, G.H., 2013. Optimising hydrological conditions to sustain wintering waterbird populations in Poyang Lake National Natural Reserve: implications for dam operations. Freshw. Biol., 58, 2366-2379.

Wellen, C., Kamran-Disfani, A.-R., Arhonditsis, G.B., 2015. Evaluation of the current state of distributed nutrient watershed-water quality modeling. Environ. Sci. Technol., 49 (6), 3278-3290.

Williams, M.R., King, K.W., Macrae, M.L., Ford, W., Van Esbroeck, C., Brunke, R.I., English, M.C., Schiff, S.L., 2015. Uncertainty in nutrient loads from tile-drained landscapes: Effect of sampling frequency, calculation algorithm, and compositing strategy. J. Hydrol., 530, 306-316.

Wu, Z.S, Cai, Y.J., Zhang, L., Chen, Y.W., 2018. Spatial and temporal heterogeneities in water quality and their potential drivers in Lake Poyang (China) from 2009 to 2015. Limnologica, 69, 115-124.

Xi, Q., 2014. Effects of land use change on nutrient export in Zhongtian River watershed based on the AnnAGNPS model. Nanjing Agricultural University, Masters Dissertation.

Xie, H., Shen, Z.Y., Chen, L., Dong, J.W., 2017. Time-varying sensitivity analysis of hydrologic and sediment parameters at multiple timescales: Implications for conservation practices. Sci. Total Environ., 598, 353-364.

Xu, H., Peng, S., 2013. Distinct effects of temperature change on discharge and non-point pollution in subtropical southern China by SWAT simulation. Hydrol. Sci. J., 58 (5), 1032-1046.

Yang, J.L., Zhang, G.L., Shi, X.Z., Wang, H.J., Cao, Z.H., Ritsema, C.J., 2009. Dynamic changes of nitrogen and phosphorus losses in ephemeral runoff processes by typical storm events in Sichuan Basin, Southwest China. Soil Tillage Res., 105 (2), 292-299.

Ye, S., Covino, T.P., Sivapalan, M., Basu, N.B., Li, H.Y., Wang, S.W., 2012. Dissolved nutrient retention dynamics in river networks: A modeling investigation of transient flows and scale effects. Water Resour. Res., 48, Art. no. W00J17.

Yin, Y.X., Jiang, S.Y., Pers, C., Yang, X.Y., Liu, Q., Jin, Y., Yao, M.X., He, Y., Luo, X.Z., Zheng, Z., 2016. Assessment of the spatial and temporal variations of water quality for agricultural lands with crop rotation in China by using a HYPE model. Int. J. Environ. Res. Public Health., 13 (3), Art. no. 336.

Zhang, W., Pueppke, S.G., Li, H., Geng, J., Diao, Y., Hyndman, D.W., 2019. Modeling phosphorus sorces and transport in a headwater catchment with rapid agricultural expansion. Environ. Pollut., 255, 113273.

Zhang, Q., Ye, X.C, Werner, A.D., Li, Y.L., Li, X.H., Xu, C-Y., 2014. An investigation of enhanced recessions in Poyang Lake: Comparison of Yangtze River and local catchment impacts. J. Hydrol., 517, 425-434.

CRediT author statement

Sanyuan Jiang: Conceptualization, Methodology, Model setup, Writing – Original Draft. **Qi Zhang**: Supervision, Writing- Reviewing. **Adrian D. Werner**: Supervision, Visualization, Writing- Reviewing and Editing. **Christopher Wellen**: Writing- Reviewing and Editing. **Peng Hu**: Data Curation. **Jinhua Sun**: Supervision. **Yanqing Deng**: Data collection. **Michael Rode**: Supervision, Visualization, Writing- Reviewing and Editing.

Figure captions

Figure 1. The Le An River catchment, showing: (a) location; (b) topography, stream network, meteorological stations, sewage treatment plants, discharge gauging stations (WK-Wang Kou, SD-San Du, XT-Xiang Tun, YS-Yin Shan, HS-Hu Shan, and SZJ-Shi Zhen Jie), water quality monitoring stations (WQ1-WQ6; note that WQ3 and WQ6 have the same locations as corresponding stream flow gauging stations XT and SZJ), and boundaries of sub-catchments delineated using water quality monitoring stations; (c) land use; (d) soils.

Figure 2. Stream TP and DP concentrations observed from water quality monitoring stations WQ1-WQ6. Note differences in vertical axis scales between sub-plots.

Figure 3. Concentration-discharge relationships for TP, DP and PP at the stations WQ3 and WQ6. P concentrations and discharge have the units of mg/L and m^3/s, respectively.

Figure 4. Simulated and observed daily discharge together with daily precipitation during the calibration period (1 Jan 1978 - 31 Dec 1982) and the first validation period (1 Jan 1983 - 31 Dec 1986) at six gauging stations.

Figure 5. Simulated and observed daily discharge together with daily precipitation at discharge gauging stations: (a) Xiang Tun, (b) Hu Shan and (c) Shi Zhen Jie during the second validation period (1 Jan 2009 - 31 Dec 2011).

Figure 6. Comparison of simulated and observed stream TP concentrations in Le An River catchment for the period 1 Jan 2009 - 31 Dec 2011, red dots highlight the underestimation of TP concentrations.

Figure 7. Comparison of simulated and observed average monthly TP loads during 2009-2011 at the catchment outlet (station Shi Zhen Jie).

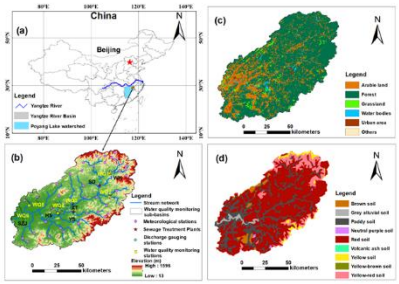

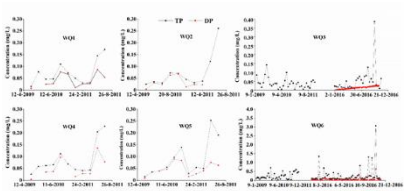

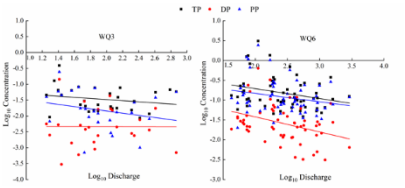

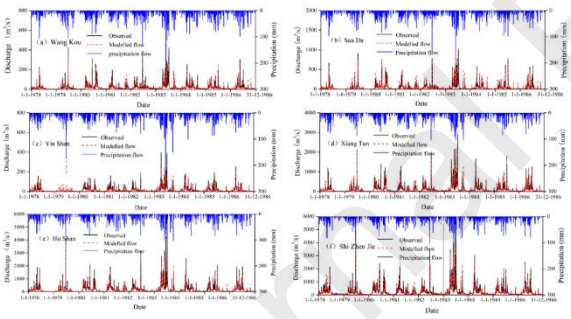

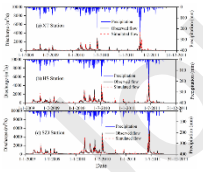

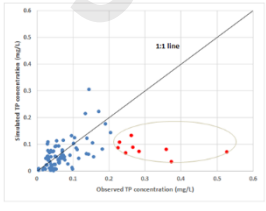

Table 1. Summary of physiographic and land use characteristics of the Le An River catchment. Hilly/mountainous areas and plains region are those at elevations greater or less than (respectively) 90 m.

Characteristics	Categories (% area)
Topography (% coverage)	Mountainous areas: 90 – 1596 m (70%), Plains region: 13 – 90 m (30%)
Land use (% coverage)	Forest (74.5%), arable land (19.0%), grassland (2.6%), urban area (1.6%), water bodies (1.6%), others (0.7%)
Soil (texture, % coverage)	Red soil (loam and clay, 64.0%), paddy soil (silty clay, 18.4%), yellow-red soil (clay and loam, 10.5%), brown soil (loam, 2.4%), yellow soil (loam and clay, 2.1%), grey alluvial soil (loam and clay, 1.5%), yellow-brown soil (loam, 0.4%), volcanic ash soil (clay, 0.5%), neutral purple soil (silty clay loam, 0.2%)
Arable land (% coverage)	Paddy field (79.0%), dry land (17.5%), vegetable land (3.5%)

Table 2. Available stream flow and stream P measurements in the Le An River catchment. See Figure 1 for station locations.

Variables	Stations	Frequency	Parameters	Period
Stream flow	Wang Kou, San Du, Yin Shan	Daily	Discharge (m^3/s)	1977-1986
	Xiang Tun, Hu Shan, and Shi Zhen Jie	Daily	Discharge (m^3/s)	1977-1986 2009-2011
Stream P concentration	WQ1, WQ2, WQ5	Three-monthly	TP, DP (mg/L)	2009-2011
	WQ3, WQ4, WQ6	Monthly	TP (mg/L)	2009-2011
	WQ3, WQ6	Biweekly to weekly	TP, DP (mg/L)	2016

Table 3. Physical meaning, initial value and range, RCS (Relative Composite Sensitivity), and optimized value of the HYPE parameters for simulating flow and P transport in the Le An River catchment.

Parameter	Categories	Initial value	Range	RCS ×1000	Calibrated value
Hydrological-process parameters					
rrcs1 – Recession coefficient for runoff in the uppermost soil layer (1/d)	Red soil	0.28	0.01-1.0	3.17	0.748
	Paddy soil	0.10	0.01-1.0	0.46	0.366
srrcs – Recession coefficient for saturation-excess surface runoff (1/d)	Arable land	0.12	0.1-1.0	0.38	0.10
	Forest	0.12	0.1-1.0	0.56	0.242
	Grassland	0.30	0.1-1.0	0.07	0.262
	Urban area	0.40	0.1-1.0	0.20	0.114
rivvel – Maximum velocity in the stream channel (m/s)		2.47	0.01-10	2.65	1.58
rcgrw – Recession coefficient for regional groundwater flow (1/d)		0.10	0.001-1.0	0.91	0.026
mperc – Maximum percolation capacity (mm/d)	Red soil	4.0	0.001-100	2.9	18.12
	Paddy soil	2.7	0.001-100	0.009	0.01
Phosphorus-process parameters					
wprod – Production/decay of P in water (kg/m^3/d)		0.002	0.001-1.0	10.70	0.0027
minerfp – Degradation of fastP to SP (1/d)	Arable land	0.50	0.00001-1.0	1.97	0.55
	Forest	0.0003	0.00001-1.0	43.19	0.0005
freund1 – Coefficient in the Freundlich equation (1/kg)	Red soil	190	10-250	101.08	189.98
	Paddy soil	50	10-250	50	12.78
freund2 – Exponent in the Freundlich equation (-)	Red soil	1.1	0.55-1.65	166.04	1.65
	Paddy soil	0.75	0.38-1.13	42.34	1.0
freund3 – Parameter that controls the adsorption/desorption velocity (1/d)	Red soil	0.50	0.25-0.75	17.23	0.75
	Paddy soil	0.009	0.005-0.014	0.17	0.005
sreroexp – Exponent in the equation for the calculation of surface runoff erosion (-)		2.26	1.5-2.6	666	2.28

Table 4. Statistical summary of stream P (TP, DP, PP) concentrations for monitoring stations WQ1-WQ6 and land use characteristics of the corresponding sub-basins.

Site	Sub-basin area (km^2)	Land use percentage (%)			TP concentration (mg/L)		DP concentration (mg/L)		PP concentration (mg/L)	
		Forest	Arable land	Urban area	Range	Mean	Range	Mean	Range	Mean

WQ1	18.96	92.5	4.4	0.9	0.015-0.172	0.072	0.007-0.087	0.041	0.003-0.118	0.031
WQ2	37.96	91.3	8.7	0	0.025-0.262	0.073	0.004-0.068	0.031	0.006-0.031	0.012
WQ3	51.09	74.5	18.5	2.3	0.005-0.386	0.046	0.001-0.143	0.012	0.0007-0.243	0.040
WQ4	112.67	60.9	33.8	1.3	0.025-0.228	0.087	0.004-0.135	0.051	0.012-0.151	0.041
WQ5	157.64	58.4	35.3	3.2	0.015-0.253	0.087	0.008-0.089	0.049	0.0004-0.178	0.043
WQ6	184.43	29.7	49.9	5.2	0.020-3.061	0.256	0.003-0.634	0.052	0.02-2.427	0.223

Table 5. Statistic model performance (daily discharge) for the calibration period (1 Jan 1978 - 31 Dec 1982) and first validation period (1 Jan 1983 - 31 Dec 1986) at six discharge gauging stations (Wang Kou, San Du, Yin Shan, Xiang Tun, Hu Shan and Shi Zhen Jie); and for the second validation period (1 Jan 2009 - 31 Dec 2011) at three discharge gauging stations (Xiang Tun, Hu Shan, and Shi Zhen Jie). *PBIAS* has the unit of %, while other variables are unitless.

Station	**Upstream area (km^2)**	**Calibration**			**First validation period**		
		NSE	***RSR***	***PBIAS***	***NSE***	***RSR***	***PBIAS***
Wang Kou	581	0.86	0.37	-10.1	0.80	0.44	-8.6
San Du	1407	0.89	0.33	5.6	0.82	0.42	14.5
Yin Shan	471	0.88	0.35	-10.2	0.84	0.40	-6.9
Xiang Tun	3878	0.92	0.29	4.2	0.88	0.35	2.5
Hu Shan	6348	0.90	0.32	-0.4	0.87	0.36	-0.2
Shi Zhen Jie	8324	0.84	0.40	-5.1	0.87	0.36	-2.6
					Second validation period		
Xiang Tun	3878				0.73	0.52	-2.7
Hu Shan	6348				0.91	0.33	-3.0
Shi Zhen Jie	8324				0.92	0.34	-5.4

Table 6. Simulated (Sim) and observed (Obs) TP, DP and PP yields (kg/ha) for 2016 from the upstream areas (above station WQ3), lowland plains region (areas between WQ3 and WQ6), and

whole catchment showing different physiographic characteristics (area, elevation, slope and land use).

Site	Area (km^2)	Average elevation (m)	Average slope (%)	Land use (%)			TP (kg/ha)		DP (kg/ha)		PP (kg/ha)	
				Forest	Arable land	Urban area	Sim	Obs	Sim	Obs	Sim	Obs
Upstream areas	3878	220	20.4	86.8	9.7	0.9	0.88	0.71	0.18	0.43	0.48	0.26
Lowland plains region	4435	132	12.9	63.8	27.2	2.2	4.69	3.19	2.15	0.87	2.55	2.54
Whole catchment	8324	176	16.6	74.5	19.0	1.6	2.91	2.03	1.33	0.66	1.58	1.47

Highlights:

- P export in mixed land use, subtropical catchment simulated using HYPE;
- P export is mainly driven by surface runoff erosion and adsorption/desorption;
- Point inputs led to elevated stream TP concentrations in low-flow conditions;
- Storm events during March-August account for most of the annual TP export.